LETTERS
PUBLISHED ONLINE: 20 JUNE 2016 | DOI: 10.1038/NCLIMATE3058
nature climate change

Role of volcanic and anthropogenic aerosols in the recent global surface warming slowdown

Doug M. Smith*, Ben B. B. Booth, Nick J. Dunstone, Rosie Eade, Leon Hermanson, Gareth S. Jones, Adam A. Scaife, Katy L. Sheen and Vikki Thompson

The rate of global mean surface temperature (GMST) warming has slowed this century despite the increasing concentrations of greenhouse gases. Climate model experiments[1–4] show that this slowdown was largely driven by a negative phase of the Pacific Decadal Oscillation (PDO), with a smaller external contribution from solar variability, and volcanic and anthropogenic aerosols[5,6]. The prevailing view is that this negative PDO occurred through internal variability[7–11]. However, here we show that coupled models from the Fifth Coupled Model Intercomparison Project robustly simulate a negative PDO in response to anthropogenic aerosols implying a potentially important role for external human influences. The recovery from the eruption of Mount Pinatubo in 1991 also contributed to the slowdown in GMST trends. Our results suggest that a slowdown in GMST trends could have been predicted in advance, and that future reduction of anthropogenic aerosol emissions, particularly from China, would promote a positive PDO and increased GMST trends over the coming years. Furthermore, the overestimation of the magnitude of recent warming by models is substantially reduced by using detection and attribution analysis to rescale their response to external factors, especially cooling following volcanic eruptions. Improved understanding of external influences on climate is therefore crucial to constrain near-term climate predictions.

The recent slowdown in surface temperature warming is clearly seen in observed time series of 15-year global mean surface temperature (GMST) trends[8,9] that reached a peak in the 15-year period 1992–2006 followed by a sharp decline (black curves in Fig. 1a). This is seen in all of the leading observational data sets despite recent claims that the slowdown is eliminated by corrections to sea surface temperature biases[12]. A similar peak and decline is also simulated by all coupled models from the Fifth Coupled Model Intercomparison Project (CMIP5, coloured curves in Fig. 1a, with thick red curve showing the ensemble mean, see Methods and Supplementary Table 1). Similar results are obtained for different trend lengths (Supplementary Fig. 1). The modelled trends are generally larger than observed. This is an important point that will be addressed later, but we first investigate the cause of the simulated peak and decline in GMST trends.

Since internal variability is unlikely to be in phase in the CMIP5 model simulations, any common signals are likely to be externally forced. We therefore investigate additional CMIP5 model simulations that are forced by different combinations of external factors (Supplementary Table 1 and Methods). These show that the sharp peak in the trend in the period 1992–2006 is caused by natural factors (Nat, green curve in Fig. 1b), and in particular the eruption of Mount Pinatubo as pointed out previously[9,13]. The reason is straightforward: the eruption of Mount Pinatubo in 1991 caused

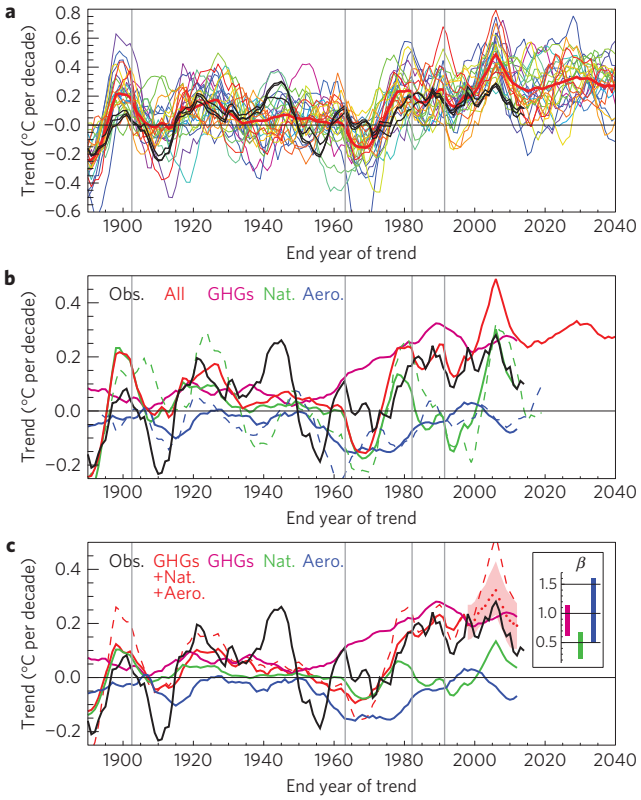

Figure 1 | Time series of 15-year trends (°C per decade) in global mean near-surface temperature. a, Observations (Obs., black line) compared with CMIP5 coupled model simulations (coloured lines, with ensemble mean in thick red; models are detailed in Supplementary Table 1). Observations are shown from the three leading data sets (Methods). The year represents the end of the 15-year trend period. Vertical grey lines indicate major volcanic eruptions. **b**, Observations (black line, average of the three data sets) compared with CMIP5 model simulations of the effects of all external forcing factors (All, red), greenhouse gases (GHGs, magenta), natural factors (volcanoes and solar variations, Nat., green) and anthropogenic aerosols (Aero., blue). The green and blue dashed curves show the HadGEM2-ES ensemble mean (Methods). **c**, The same as in **b**, but rescaled on the basis of total least-squares multiple linear regression between observations up to 1998 and the three predictors GHGs, Nat., and Aero. (Methods). The 95% confidence interval of the resulting scaling factors (β) is shown inset. Dashed and solid red curves show the unscaled and scaled combinations respectively. The dotted red curve (with shading representing the 95% confidence interval) shows the prediction that would have been made in 1998.

Met Office Hadley Centre, FitzRoy Road, Exeter EX1 3PB, UK. *e-mail: doug.smith@metoffice.gov.uk

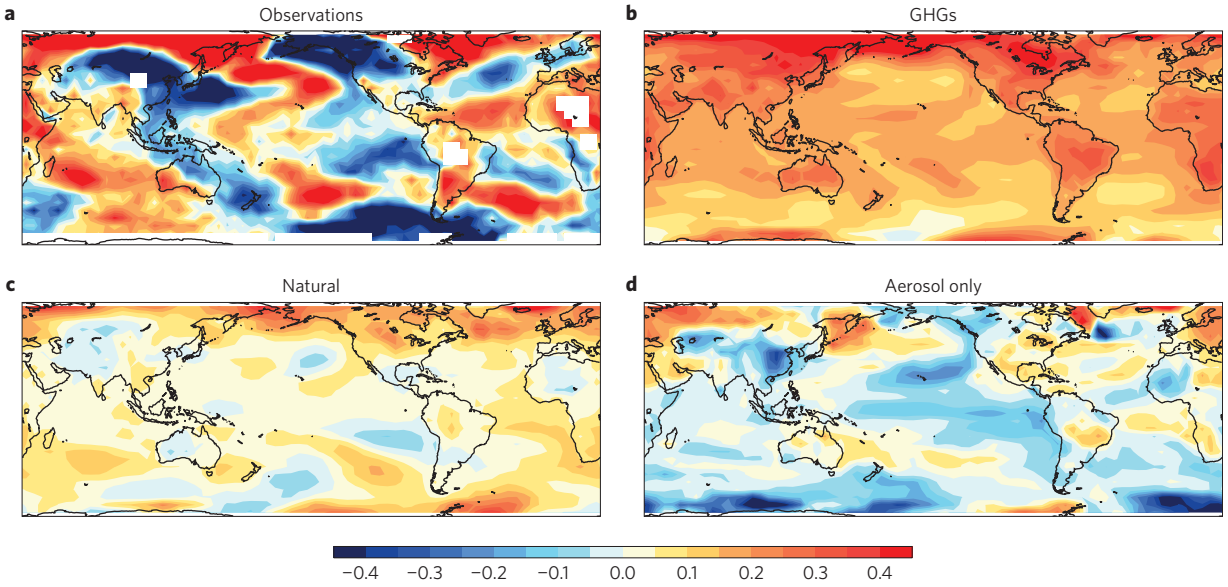

Figure 2 | Near-surface temperature trends for the 15-year period 1998 to 2012. a–d, Observations (**a**, averaged over the three data sets) are compared with CMIP5 model simulations of the effects of GHGs (**b**) natural factors (volcanoes and solar variations) (**c**) and anthropogenic aerosols (**d**). Units are °C per decade.

simulated global temperatures to cool in 1992, leading to a peak warming trend for the period following this cool year (1992–2006), and hence a subsequent reduction in trends for more recent periods (Supplementary Fig. 1).

Importantly, however, anthropogenic aerosols have also contributed to the simulated GMST slowdown, shown by increasing cooling trends in the Aero simulations for 15-year periods ending after about 2000 (blue curve in Fig. 1b, see Methods and Supplementary Figs 1 and 2). Many studies[1–4,11] have shown that temperature trends in the Pacific towards a negative phase of the Pacific Decadal Oscillation (PDO) were key for driving the observed slowdown over the most recent 15 to 20 years. We therefore further investigate the simulated GMST slowdown by examining the spatial patterns of trends for the period 1998–2012 (the most recent 15-year period available because the CMIP5 model simulations with different forcing combinations end in 2012). Trends from greenhouse gases and natural factors (Fig. 2b,c) bear little resemblance to the observations (Fig. 2a). However, anthropogenic aerosols (Fig. 2d) drive a pattern of trends in the Pacific towards a negative PDO similar to (but weaker than) the observations, with cooling in the eastern tropical Pacific and extending along the western coasts of North and South America and warming in the central North and South Pacific. This pattern is shown to be robust by further analysis in which the effects of anthropogenic aerosols are diagnosed in different ways (Methods and Supplementary Fig. 3). The observed shift towards a negative PDO involved changes in atmospheric circulation including strengthened Pacific trade winds[2,3] and weakened Aleutian Low[4,14]. These are also simulated by the models in response to anthropogenic aerosols (Fig. 3 and Supplementary Figs 4 and 5), although the response is weaker than observed (discussed later). This robust model response provides strong evidence that external forcing by anthropogenic aerosols contributed to the recent negative PDO and it did not occur solely through internal variability as previously thought[4,7–11].

Changes in atmospheric circulation are driven by localized heating and/or cooling. During the GMST slowdown there were large regional changes in anthropogenic aerosol emissions with a reduction in sulfate aerosol optical depth (SAOD) over USA and Europe and an increase over China seen in both observations[15] and models (Fig. 4a). Lagged correlations between trends in the Aleutian Low (measured by the North Pacific Index, NPI[16]) and SAOD in these regions are largest when SAOD leads by a few years (Supplementary Fig. 6). This is consistent with SAOD driving changes in the Aleutian Low in these aerosol-only simulations, and suggests that the atmospheric response involves coupled changes in sea surface temperatures and land temperatures that evolve over several years. Lagged regressions also highlight SAOD changes in these same regions (China, USA and Europe) as potential drivers of Aleutian Low variability in earlier periods before the recent GMST slowdown (Fig. 4b). Furthermore, trends in the Aleutian Low tend to lead trends in the PDO (Supplementary Fig. 7). This lagged correlation analysis therefore suggests that SAOD changes drive changes in the Aleutian Low and trade winds (Supplementary Fig. 8) leading to a coupled basin-wide response in the PDO[2,3].

The correlations (Supplementary Fig. 6) show that a weakening of the Aleutian Low (an increase in the NPI) tends to be preceded by increased SAOD over China and reduced SAOD over the USA and Europe. Reduced USA/Europe emissions would be expected to warm the North Atlantic relative to the Pacific[17], thereby changing the Walker circulation and weakening the Aleutian Low consistent with mechanisms described previously[14]. A potential mechanism through which Chinese aerosol emissions affect the Aleutian Low is suggested by trends in geopotential height at 200 hPa (Z200) that show alternating highs and lows emanating from the western tropical Pacific polewards and eastwards in both hemispheres (Fig. 3e,f). This is consistent with Rossby waves[4] excited by changes in western Pacific upper tropospheric divergent flow that are driven by aerosol changes[18–20]. Indeed, models simulate trends in Rossby wave source over China and east of Japan similar to observations (Supplementary Fig. 9), and long-wavelength Rossby waves propagate northeastwards from the latter region, in qualitative agreement with trends in geopotential height and the Aleutian Low (Fig. 3e,f, green dots). Our conclusion that increased Chinese aerosol emissions drive a weakening of the Aleutian Low agrees with dedicated coupled model experiments[21], but not with a previous study linking the strengthening of the Aleutian Low between the 1960s and the 1990s with increased Chinese aerosol emissions[22]. We suggest that increases in aerosol emissions over the USA during this period (Fig. 4c) may have played a role, confusing

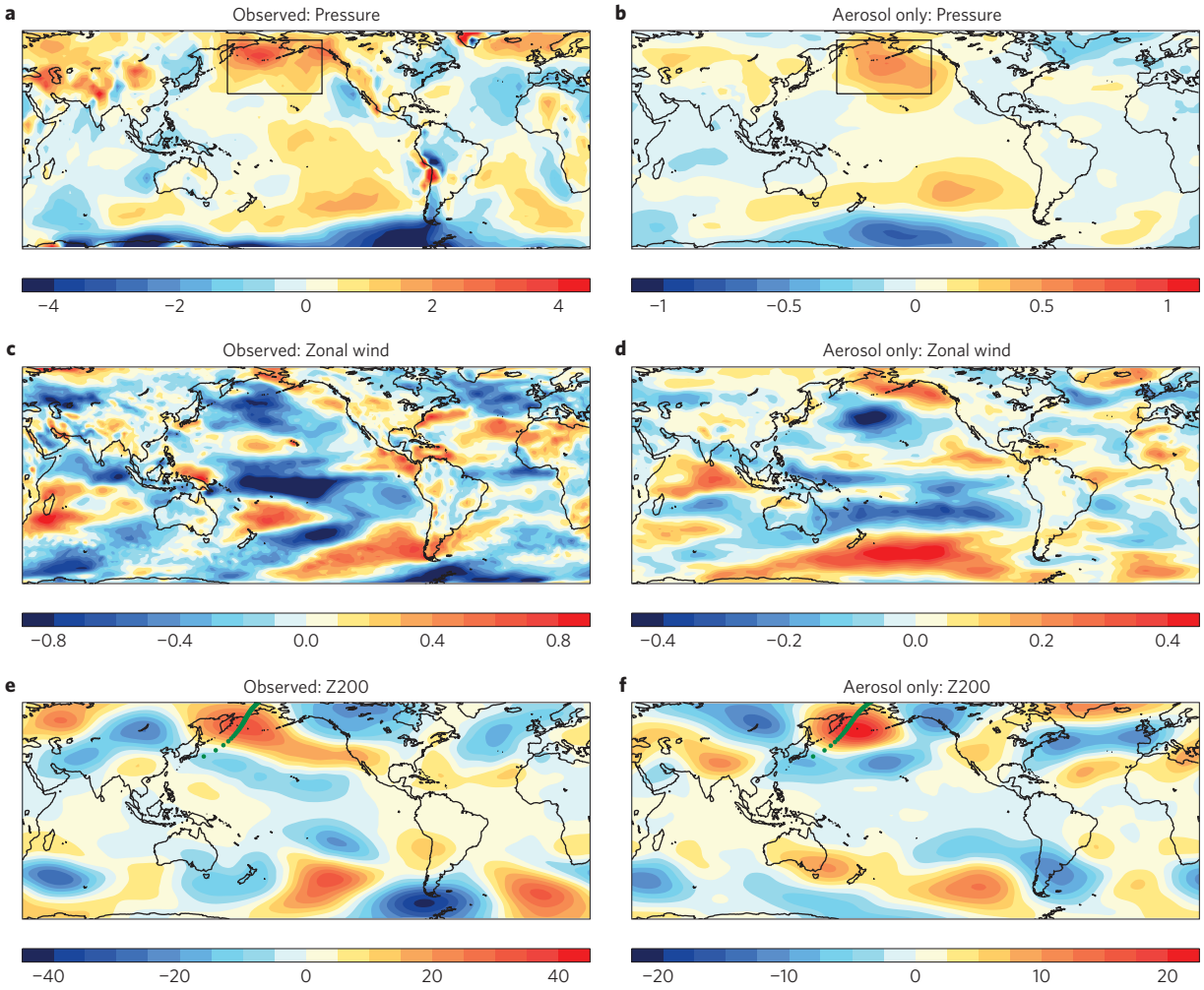

Figure 3 | Anthropogenic aerosol impacts on atmospheric circulation trends for the 15-year period 1998 to 2012. a–f, Observed trends (**a**,**c**,**e**) are compared with CMIP5 model simulations driven only by anthropogenic aerosols (**b**,**d**,**f**) for sea level pressure (top row, hPa per decade), surface zonal wind (middle row, m s^{-1} per decade) and geopotential height (December to February) at 200 hPa (bottom row, m per decade). Note the different scale bars between observations and models. The boxes in **a**,**b** show the Aleutian Low region (160°–220° E, 30°–65° N) measured by the NPI[16]. Zonal winds are based on 11 model simulations since data were not available for CSIRO-Mk3-6-0. Geopotential height is from the ensemble mean of HadGEM2-ES since data were not available for the other models. Green dots in **e**,**f** show the propagation of wavenumber 2 Rossby waves from the source east of Japan (Supplementary Fig. 9).

this earlier interpretation. However, further studies are needed to understand the physical processes in more detail.

Changes in aerosol emissions were smaller during the first half of the twentieth century than the second, especially over China (Fig. 4c). Observed changes in NPI trends before 1950 therefore do not appear to be strongly related to anthropogenic aerosols and may have occurred through internal variability. However, the timing of changes in NPI trends since the 1960s is captured very well by the Aero simulations, suggesting that internal variability was modulated by changes in external forcing. Other studies have also shown modulations of internal variability by external forcing from volcanic and anthropogenic aerosols, including for example El Niño[23], the Atlantic Multidecadal Oscillation[17] and recent 30-year or longer trends in the PDO[24,25]. This is important for reconciling our results with previous evidence that the GMST slowdown occurred largely through internal variability, and will be discussed further below.

The HadGEM2-ES aerosol and Nat simulations extend until 2020, enabling future projections to be investigated. Over the period 2005 to 2020 Chinese aerosol emissions reduce rapidly in the RCP8.5 scenario in line with air quality improvements, and HadGEM2-ES simulates a rapid strengthening of the Aleutian Low and increasing GMST trends (blue dashed curves in Figs 1b and 4c). Recent analyses and satellite observations[15] show a decline in Chinese aerosol emissions since 2006 consistent with this scenario, and the observed Aleutian Low now shows a marked strengthening (Fig. 4c). Furthermore, the GMST response to natural factors is projected to return to neutral as the effects of Pinatubo recede (Fig. 1b, green dashed curve). The external factors that contributed to the GMST slowdown therefore appear to be diminishing or reversing. Barring a major volcanic eruption, and assuming continued aerosol mitigation especially in China, this suggests that GMST trends may increase rapidly over the coming few years.

Our results suggest that a slowdown in GMST trends could have been predicted in advance following the eruption of Mount Pinatubo and assuming that changes in anthropogenic aerosol emissions could have been anticipated. However, although the models simulate a reduction in GMST trends, they tend to overestimate the magnitude of the trends since about 2000 (Fig. 1a). This overestimation might be due to internal variability, but it is also possible that the magnitude of the response to different forcing factors is not simulated perfectly by the models. We explore this further by performing a detection and attribution

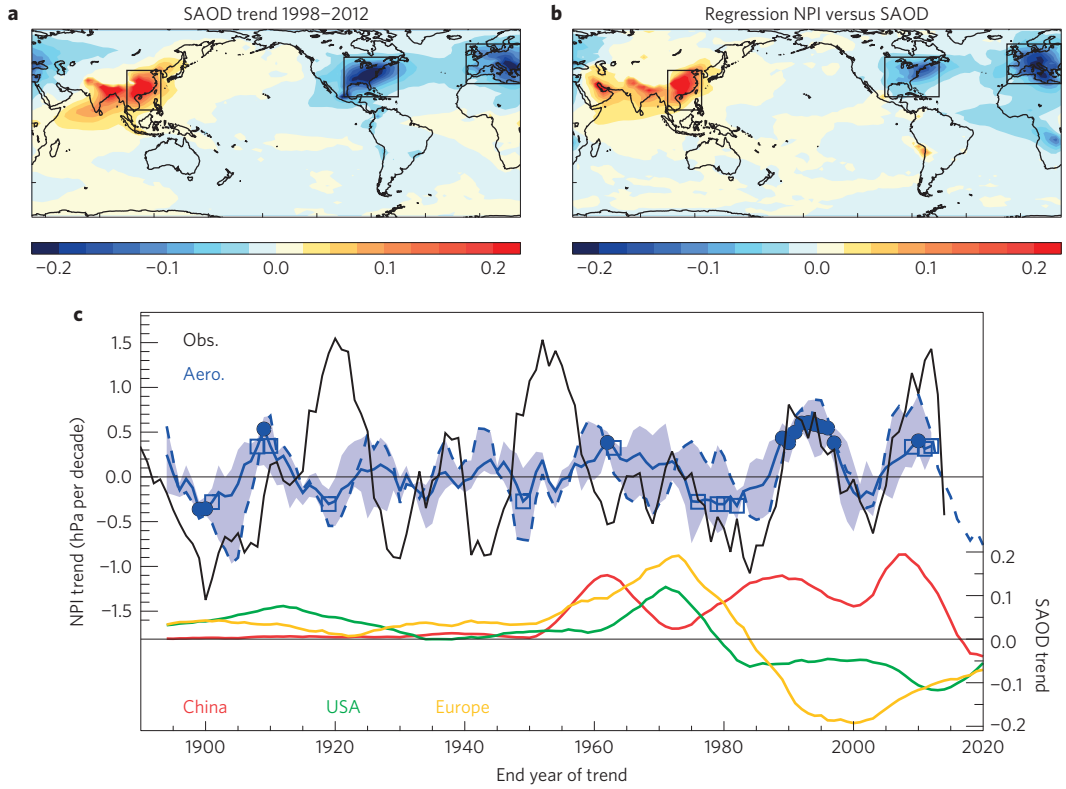

Figure 4 | Influence of sulfate aerosols on the Aleutian Low. a, Sulfate aerosol optical depth (SAOD) trend (hPa per decade) for the period 1998–2012. **b**, Linear regression (hPa per decade) between NPI[16] and SAOD three years earlier from the Aero. simulations using data before 1998. **c**, Time series of rolling 15-year trends in the NPI from observations (black line) and the ensemble-mean aerosol only simulations (blue line, solid curve shows ensemble mean with shading showing the range from the three models that provided ensemble simulations CSIRO-Mk3-6-0, CanESM2 and HadGEM2-ES, Supplementary Table 1), along with SAOD trends over China (red), USA (green) and Europe (orange). Circles (squares) show where values are significant at $p = 0.05$ (0.1, Methods). The dashed blue curve shows the HadGEM2-ES ensemble mean. SAOD values are the ensemble mean of the HadGEM2-ES aerosol simulations. Boxes for China (100°–125° E, 10°–40° N), USA (260°–300° E, 20°–50° N) and Europe (10° W–30° E, 30°–60° N) are shown in **a**,**b**.

analysis of GMST trends using GHG, Nat and Aero model simulations and observations, using data up to 1998 so that the recent GMST slowdown is excluded (Methods). This yields scaling coefficients (β) that are significantly greater than zero (Fig. 1c inset panel) suggesting a detectable influence from all three factors. Scaling coefficients are consistent with unity for GHG and Aero (0.62–1.13 and 0.49–1.60 respectively, 95% confidence), but significantly smaller for Nat (0.22–0.67) consistent with previous studies suggesting a potential overestimation of cooling following volcanoes[9,26]. Analysing global annual mean temperature (Supplementary Fig. 10), and considering different periods, trend lengths and the potential coincidence of El Niño and volcanoes[13,27] gives similar overall conclusions (Supplementary Table 2), although there are uncertainties in the scaling coefficients.

Applying the scaling coefficients produces a forecast from 1998 that is in much better agreement with the subsequent observations for both trends and annual mean GMST (compare red dashed and dotted curves in Fig. 1c and Supplementary Fig. 10). Errors are also reduced for other observational periods and trend lengths (Supplementary Table 2). The forecast is improved throughout, with the largest improvement seen for the peak trend over the period 1992–2006 following the eruption of Mount Pinatubo. Over the most recent period (1998–2012) the difference between forecast and observations is nearly halved, but the observations remain below the forecast 95% confidence interval. However, the forecast does not take into account several minor volcanic eruptions and an extended and deeper solar minimum, both of which reduced GMST over this period[5,6]. Furthermore, although the Aero ensemble captures the timing of recent changes in Aleutian Low trends, their magnitude appears to be underestimated, especially for the minimum in 1985 and the recent maximum in 2012 (Figs 3 and 4c). This could be because internal variability might have reinforced the aerosol signal in reality by coincidence[25]. However, aerosol interactions with climate are complex: aerosols directly alter the short-wave radiation, but also have important indirect effects by changing cloud albedo and lifetime. Although indirect effects are included in the aerosol simulations presented here, the magnitude of the response is uncertain since it depends on the implementation schemes and the fidelity of the model cloud simulations[28], and also the remote dynamical response (Supplementary Fig. 4). Given the spread in the three model ensembles analysed here (blue shading in Fig. 4c and Supplementary Fig. 4), uncertainties in the simulation of aerosol affects might also help to explain the remaining differences between models and observations.

We have shown that a slowdown in recent GMST trends, with timing and magnitude very similar to observations, is simulated by the ensemble mean of CMIP5 coupled models, suggesting a potentially important role for external forcing. The simulated GMST slowdown is driven initially by the recovery from the eruption of Mount Pinatubo in 1991[9,13], and more recently by a shift in anthropogenic aerosol emissions from USA to China that drives a negative PDO. This is different to previous studies[5,6] that highlighted external forcing from minor volcanic eruptions and an extended solar minimum since these factors are not included in the CMIP5 simulations. Furthermore, the globally averaged trend in SAOD over the period 1998–2012 is small (−0.005 per decade), consistent with observations[29]. Hence, anthropogenic aerosols affect the GMST slowdown by modulating the PDO rather than by a globally

averaged forcing as suggested previously[30]. Our results imply that the GMST slowdown could have been predicted in advance, but the model trends are generally larger than observed. However, models may not respond perfectly to external factors, and agreement with observations is greatly improved by rescaling the different factors on the basis of detection and attribution analysis. We stress that statistical scaling factors are uncertain (Supplementary Table 2) and should be interpreted with caution. Nevertheless, our results show that much of the difference between models and observations is potentially explained by uncertainties in the response to external factors. Hence, improved understanding of external influences on climate is urgently needed to constrain future predictions.

Our results provide an alternative explanation to the prevailing view that internal variability played a key role in the GMST slowdown. The prevailing arguments are: internal variability is expected to cause GMST slowdown periods, and does so in coupled model simulations[6–8,10]; the PDO played a key role, and is normally associated with internal variability[1,4,11], and recent PDO variability was not driven by changes in greenhouse gases[3]; and the difference between observed and modelled 15-year trends during the GMST slowdown is consistent with internal variability assessed over the whole period since 1900[9]. Although this evidence is plausible it is circumstantial and does not necessarily prove that internal variability played a major role over the actual period in question. Instead, the model simulations presented here strongly suggest that the phase of the PDO during the GMST slowdown was modulated by external forcing from anthropogenic aerosols. This is fundamental for understanding and attributing past climate change and for predicting both regional and global climate in the coming years to decades. To quantify the roles of internal variability and external forcing completely would require a perfect knowledge of the forced response, which is not possible with imperfect models and imperfect estimates of the forcing. Hence, we cannot determine whether the remaining differences between model simulations and observations are due to model imperfections or coincidental reinforcement of the externally forced signal by internal variability. However, model projections suggest an impending reversal to a positive phase of the PDO and increased GMST trends if aerosol emissions from China continue to reduce, providing an opportunity to further assess aerosol impacts on climate.

Methods

Methods and any associated references are available in the online version of the paper.

Received 3 March 2016; accepted 9 May 2016;
published online 20 June 2016

References

1. Kosaka, Y. & Xie, S.-P. Recent global-warming hiatus tied to equatorial Pacific surface cooling. *Nature* **501,** 403–407 (2013).
2. England, M. H. *et al*. Recent intensification of wind-driven circulation in the Pacific and the ongoing warming hiatus. *Nature Clim. Change* **4,** 222–227 (2014).
3. Watanabe, M. *et al*. Contribution of natural decadal variability to global warming acceleration and hiatus. *Nature Clim. Change* **4,** 893–897 (2014).
4. Trenberth, K. E., Fasullo, J. T., Branstator, G. & Phillips, A. S. Seasonal aspects of the recent pause in surface warming. *Nature Clim. Change* **4,** 911–916 (2014).
5. Schmidt, G. A., Shindell, D. T. & Tsigaridis, K. Reconciling warming trends. *Nature Geosci.* **7,** 158–160 (2014).
6. Huber, M. & Knutti, R. Natural variability, radiative forcing and climate response in the recent hiatus reconciled. *Nature Geosci.* **7,** 651–656 (2014).
7. Meehl, G. A., Arblaster, J. M., Fasullo, J. T., Hu, A. & Trenberth, K. E. Model-based evidence of deep-ocean heat uptake during surface-temperature hiatus periods. *Nature Clim. Change* **1,** 360–364 (2011).
8. Risbey, J. S. *et al*. Well-estimated global surface warming in climate projections selected for ENSO phase. *Nature Clim. Change* **4,** 835–840 (2014).
9. Marotzke, J. & Forster, P. M. Forcing, feedback and internal variability in global temperature trends. *Nature* **517,** 565–570 (2015).
10. Roberts, C. D., Palmer, M. D., McNeall, D. & Collins, M. Quantifying the likelihood of a continued hiatus in global warming. *Nature Clim. Change* **5,** 337–342 (2015).
11. Dai, A., Fyfe, J. C., Xie, S.-P. & Dai, X. Decadal modulation of global surface temperature by internal climate variability. *Nature Clim. Change* **5,** 555–559 (2015).
12. Karl, T. R. *et al*. Possible artifacts of data biases in the recent global surface warming hiatus. *Science* **348,** 1469–1472 (2015).
13. Santer, B. D. *et al*. Volcanic contribution to decadal changes in tropospheric temperature. *Nature Geosci.* **7,** 185–189 (2014).
14. McGregor, S. *et al*. Recent Walker circulation strengthening and Pacific cooling amplified by Atlantic warming. *Nature Clim. Change* **4,** 888–892 (2014).
15. Klimont, Z., Smith, S. J. & Cofala, J. The last decade of global anthropogenic sulfur dioxide: 2000–2011 emissions. *Environ. Res. Lett.* **8,** 014003 (2013).
16. Trenberth, K. E. & Hurrell, J. W. Decadal atmosphere-ocean variations in the Pacific. *Clim. Dynam.* **9,** 303–319 (1994).
17. Booth, B. B. B., Dunstone, N. J., Halloran, P. R., Andrews, T. & Bellouin, N. Aerosols implicated as a prime driver of twentieth-century North Atlantic climate variability. *Nature* **484,** 228–232 (2012).
18. Bollasina, M. A., Ming, Y., Ramaswamy, V., Schwarzkopf, M. D. & Naik, V. Contribution of local and remote anthropogenic aerosols to the twentieth century weakening of the South Asian monsoon. *Geophys. Res. Lett.* **41,** 680–687 (2014).
19. Ming, Y., Ramaswamy, V. & Chen, G. A model investigation of aerosol-induced changes in boreal winter extratropical circulation. *J. Clim.* **24,** 6077–6091 (2011).
20. Lewinschal, A., Ekman, A. M. L. & Krnich, H. The role of precipitation in aerosol-induced changes in northern hemisphere wintertime stationary waves. *Clim. Dynam.* **41,** 647–661 (2012).
21. Yeh, S.-W. *et al*. Changes in the variability of the North Pacific sea surface temperature caused by direct sulfate aerosol forcing in China in a coupled general circulation model. *J. Geophys. Res.* **118,** 1261–1270 (2013).
22. Boo, K.-O. *et al*. Influence of aerosols in multidecadal SST variability simulations over the North Pacific. *J. Geophys. Res.* **120,** 517–531 (2015).
23. Maher, N., McGregor, S., England, M. H. & Gupta, A. S. Effects of volcanism on tropical variability. *Geophys. Res. Lett.* **42,** 6024–6033 (2015).
24. Allen, R. J., Norris, J. R. & Kovilakam, M. Influence of anthropogenic aerosols and the Pacific Decadal Oscillation on tropical belt width. *Nature Geosci.* **7,** 270–274 (2014).
25. Dong, L., Zhou, T. & Chen, X. Changes of Pacific decadal variability in the twentieth century driven by internal variability, greenhouse gases, and aerosols. *Geophys. Res. Lett.* **41,** 8570–8577 (2014).
26. Schurer, A. P., Hegerl, G. C., Mann, M. E., Tett, S. F. B. & Phipps, S. J. Separating forced from chaotic climate variability over the past millennium. *J. Clim.* **26,** 6954–6973 (2013).
27. Lehner, F., Schurer, A. P., Hegerl, G. C., Deser, C. & Frolicher, T. L. The importance of ENSO phase during volcanic eruptions for detection and attribution. *Geophys. Res. Lett.* **43,** 2851–2858 (2016).
28. Wilcox, L. J., Highwood, E. J., Booth, B. B. B. & Carslaw, K. S. Quantifying sources of inter-model diversity in the cloud albedo effect. *Geophys. Res. Lett.* **42,** 1568–1575 (2015).
29. Murphy, D. M. Little net clear-sky radiative forcing from recent regional redistribution of aerosols. *Nature Geosci.* **6,** 258–262 (2013).
30. Kaufmann, R. K., Kauppi, H., Mann, M. L. & Stock, J. H. Reconciling anthropogenic climate change with observed temperature 1998–2008. *Proc. Natl Acad. Sci. USA* **108,** 11790–11793 (2011).

Acknowledgements

This work was supported by the Joint DECC/Defra Met Office Hadley Centre Climate Programme (GA01101), and the EU FP7 SPECS project. We acknowledge the World Climate Research Programme's Working Group on Coupled Modelling, which is responsible for CMIP, and we thank the climate modelling groups for producing and making available their model outputs.

Author contributions

D.M.S. led the analysis and writing, with suggestions and comments from all authors. G.S.J. guided the detection and attribution analysis.

Additional information

Supplementary information is available in the online version of the paper. Reprints and permissions information is available online at www.nature.com/reprints. Correspondence and requests for materials should be addressed to D.M.S.

Competing financial interests

The authors declare no competing financial interests.

Methods

Model simulations. We use coupled climate model simulations from the Fifth Coupled Model Intercomparison Project (CMIP5), together with additional Hadley Centre simulations with HadGEM2-ES (Supplementary Table 1). The effects of different external forcing factors were investigated by considering simulations forced by: all factors (All, 65 simulations); anthropogenic greenhouse gases (GHGs, 35 simulations); natural solar variations and volcanic eruptions (Nat, 38 simulations); anthropogenic land use changes (LU, 19 simulations); anthropogenic aerosols (Aero, 15 simulations); anthropogenic ozone (Oz, 10 simulations); all anthropogenic factors (Anthro = GHGs + Aero + LU + Oz); all except anthropogenic aerosols (NoAero, 8 simulations); all except anthropogenic ozone (NoOz, 5 simulations). We extend the historical simulations using the RCP4.5 scenario (RCP8.5 for HadGEM2-ES Aero). Simulations with different forcing factors end in 2012 except HadGEM2-ES, which extend to 2020. We compute rolling 15-year trends, and average all of the simulations with equal weight regardless of the model. We diagnose the effects of anthropogenic aerosols in four different ways: Aero; All-NoAero; All-Nat-GHG-LU-Oz; Anthro-GHG-LU-Oz. For Oz we use the average of Oz and All-NoOz.

Significance. To compute the significance of externally forced signals we compare them against control integrations, which have no inter-annual variations in external forcing. We use the latest 300 years of control integrations, linearly detrended to remove drift. We compute confidence intervals from a sample of 10,000 ensemble-mean 15-year trends, with ensemble size equal to the externally forced simulations. Values are randomly drawn by bootstrapping with replacement, in blocks of 15 to account for autocorrelation.

Observations. Near-surface temperature observations are taken from the three leading data sets: HadCRUT4[31], NASA-GISS[32] and NCDC[12]. Mean sea level pressure is taken from HadSLP2[33] and zonal winds and geopotential heights are taken from ERA Interim[34].

Detection and attribution analysis. We use the total least-squares multiple linear regression detection and attribution framework[35] to compute scaling coefficients (β) relating observed 15-year GMST trends (Y_{obs}) to model GHGs, Nat and Aero simulations (F), such that

$$Y_{obs} = (F_{GHG} + \epsilon_{GHG})\beta_{GHG} + (F_{Nat} + \epsilon_{Nat})\beta_{Nat} + (F_{Aero} + \epsilon_{Aero})\beta_{Aero} + \varepsilon_{noise} \quad (1)$$

where ϵ is variability remaining after ensemble averaging, and ε_{noise} is the residual associated with internal variability computed from independent sections of the model control integrations.

References

31. Morice, C. P., Kennedy, J. J., Rayner, N. A. & Jones, P. D. Quantifying uncertainties in global and regional temperature change using an ensemble of observational estimates: the HadCRUT4 data set. *J. Geophys. Res.* **117,** D08101 (2012).
32. Hansen, J., Ruedy, R., Sato, M. & Lo, K. Global surface temperature change. *Rev. Geophys.* **48,** RG4004 (2010).
33. Allan, R. J. & Ansell, T. J. A new globally complete monthly historical gridded mean sea level pressure data set (HadSLP2): 1850–2003. *J. Clim.* **19,** 5816–5842 (2006).
34. Dee, D. P. *et al*. The ERA-Interim reanalysis: configuration and performance of the data assimilation system. *Q. J. R. Meteorol. Soc.* **137,** 553–597 (2011).
35. Allen, M. R. & Stott, P. A. Estimating signal amplitudes in optimal fingerprinting I: estimation theory. *Clim. Dynam.* **21,** 477–491 (2003).